Preparation of [Ru6N] clusters on MgO, K+/MgO, Cs+/MgO, and Al2O3 and the reactivities with H2 and N2

ARTICLE *in* THE JOURNAL OF PHYSICAL CHEMISTRY · JUNE 1995

DOI: 10.1021/j100025a041

2 AUTHORS:

Yasuo Izumi
Chiba University
125 PUBLICATIONS **1,192** CITATIONS
SEE PROFILE

Ken-ichi Aika
Japan Science and Technology Agency (JST)
196 PUBLICATIONS **4,773** CITATIONS
SEE PROFILE

Preparation of [Ru_6N] Clusters on MgO, K^+/MgO, Cs^+/MgO, and Al_2O_3 and the Reactivities with H_2 and N_2

Yasuo Izumi* and Ken-ichi Aika*

Department of Environmental Chemistry and Engineering, Interdisciplinary Graduate School of Science and Engineering, Tokyo Institute of Technology, 4259 Nagatsuta, Midori-ku, Yokohama 226, Japan

Received: January 26, 1995; In Final Form: April 3, 1995[⊗]

The supported ruthenium clusters [Ru_6N] were prepared on MgO, K^+/MgO, and Cs^+/MgO from $[Ru_6N(CO)_{16}]^-$ cluster as hydrogenation catalysts, stabilized, and chemically modified by nitrido nitrogen. The characterization and reactivities with H_2 and N_2 were investigated by EXAFS (extended X-ray absorption fine structure) in relation to their catalysis promoted by nitrido nitrogen. The [Ru_6N] cluster unit was found to remain on MgO after heating in vacuum at 813 K (decarbonylated) and in H_2 at 588 K (reaction condition of N_2 hydrogenation), whereas the $[Ru_6N(CO)_{16}]^-$ cluster strongly interacted with the Al_2O_3 surface to degrade to [Ru_3] by heating in vacuum at 813 K. The decarbonylated [Ru_6N] framework also remained in H_2 at 588 K on K^+/MgO and Cs^+/MgO without aggregation or degradation. By changing the Ru loading from 0.48 to 3.9 wt % on MgO, the coordination number $N_{Ru-O_{su}}$ (O_{su}, oxygen atom at surface) decreased from 1.2 to 0.3, while the [Ru_6N] cluster unit remained unchanged for samples with Ru loading up to ~2.5 wt %. The preferable reaction of [Ru_6N] clusters with MgO(001) flat surfaces was suggested for the sample at 2.5 wt % Ru, but the cluster should have reacted mainly with lower coordination sites of MgO for the sample with lower Ru loading (~0.5 wt %). The $r_{Ru-O_{su}}$ was shorter for [Ru_6N] on K^+/MgO and Cs^+/MgO (2.00−2.03 Å) than on MgO (2.13 Å), implying that the [Ru_6N] was interacted with O_{su} atoms bonded to K^+ or Cs^+ ions to have a direct support effect of basic oxide K^+/MgO or Cs^+/MgO on catalysis. H-induced structure changes were observed for [Ru_6N]/MgO and [Ru_6N]−Cs^+/MgO as the reversible changes on bonding distance r_{Ru-Ru} of 0.03 and 0.08 Å, respectively, by the adsorption/desorption of H_2. The adsorption of N_2 was simple adsorption on [Ru_6N] without structural change of [Ru_6N] on MgO or Cs^+/MgO.

Introduction

Metal clusters as homogeneous (in liquid) and heterogeneous (supported clusters) catalysts are expected to be effective catalysts associated with their multiple metal sites. The specific catalysis has been reported on supported carbido clusters [Ru_6C] and [Rh_6C] on MgO, La_2O_3, SiO_2, Al_2O_3, TiO_2, etc.[1-3] Supported [Ru_6C] clusters prepared from $[Ru_6C(CO)_{16}Me]^-$ produced oxygenated compounds (MeOH, H_2CO, Me_2O) from CO + H_2 with high activities and selectivities.[3] Supported [Rh_6C] clusters prepared from $[Rh_6C(CO)_{15}]^{2-}$ produced propanal from C_2H_4 + CO + H_2 in high selectivities.[2] Active structures were indicated to be carbido metal hexamers [Ru_6C] and [Rh_6C] by means of EXAFS, and electron donation from carbido carbon to the cluster framework [M_6] (M = Ru, Rh) was suggested to have a chemical effect on catalysis. In relation to the effects of structure on catalysis, reversible expansion/contraction of the [Ru_6C] framework was observed by the adsorption/desorption of CO under *in-situ* conditions (in CO + H_2 around 523 K).[1,2,4] These EXAFS results indicated that the expansion of the [Ru_6C] framework facilitated H_2 molecules to access Ru cluster sites covered with CO(a) and to dissociate by elongating the Ru−Ru distance.[1,2] As a result of this hydrogen activation, the reaction path was switched over from CO-dissociative (CH_4 formation) to CO-associative type (oxygenate formation). Similarly, propanal was selectively formed on CO-covered [Rh_6C] clusters on SiO_2.[2]

These chemical (electron donation from C) and structural (cluster framework expansion) effects found for supported [Ru_6C] and [Rh_6C] clusters implied the possibility of investigating new catalyst systems of transition metal + main group element, such as ruthenium carbide or nitride and rhodium carbide or nitride, although studies on these systems were very rare because they cannot exist as bulk in usual thermodynamic conditions. Recently, we reported the catalysis of nitrido−[Ru_6] clusters $[Ru_6N(CO)_{16}]^-$ on MgO, K^+/MgO, and Cs^+/MgO, which retained the hexamer [Ru_6N] unit in the reaction conditions. The interstitial nitrido nitrogen was suggested to promote catalysis through the comparison of activities with other supported clusters and conventional Ru catalysts.[5] Similar to the framework expansion/contraction of [Ru_6C] clusters by CO adsorption/desorption, expansion/contraction of the [Ru_6N] framework was observed by the adsorption/desorption of hydrogen. These data suggested that the catalyst systems of transition metal (Ru, Rh) + carbon or nitrogen were impossible as bulk, but possible as very small metal particles such as supported hexamer clusters + carbon or nitrogen.

The information about the interactions of supported clusters with H_2 is important in relation to catalysis (hydrogenation), but research on the interactions has been difficult because of the "invisibleness" of hydrogen to most spectroscopies and the instability of supported clusters in reaction conditions of hydrogenation. The hydrogen effect on metal particle structure was investigated for Ir/Al_2O_3 after reduction (427 K) and subsequent heating in vacuum (650 K) by means of EXAFS.[6] By heating at 650 K, the bonding distance r_{Ir-Ir} and coordination number N_{Ir-Ir} decreased from 2.71 to 2.64 Å (Å = 10^{-1} nm) and from 4.9 to 4.0, respectively. The interaction of Ir clusters with H_2 was not clear due to the change of cluster structure. It was suggested that the cluster structure was transformed from hemispherical to almost flat on the basis of the decrease of N_{Ir-Ir}. The conventional Pd/C (average Pd particle size 35 Å) and Pd/

* To whom correspondence should be addressed. E-mail: yizumi@chemenv.titech.ac.jp.

[⊗] Abstract published in *Advance ACS Abstracts,* June 1, 1995.

0022-3654/95/2099-10336$09.00/0

Al_2O_3 (34 Å) were treated in H_2 at 373 K, and subsequently the ambient gas was switched from H_2 to Ar at the same temperature.[7] During the desorption of H(a), the r_{Pd-Pd} was decreased from 2.82 to 2.76 Å (Pd/C) and from 2.82 to 2.75 Å (Pd/Al_2O_3) keeping the N_{Pd-Pd} almost unchanged. The palladium hydride PdH_x ($x \sim 0.44$) formation/decomposition on C or Al_2O_3 was suggested compared to α-phase PdH_x ($x \ll 0.6$) and β-phase PdH_x ($x \sim 0.6$) as bulk Pd hydride.

The spectroscopic detection of H(a) was reported by IR (infrared absorption) and NMR (nuclear magnetic resonance). Different from the previous reports on supported metal catalysts, multifold (bridging and 3-fold) H(a) were detected in addition to the on-top H(a) on conventional Ru/MgO and $Ru-Cs^+/MgO$ at 183 K.[8] Two peaks were observed for conventional Ru/SiO_2 around −60 ppm in H_2 (1.3−100 kPa) (α) and around −30 ppm (13−100 kPa) (β) by solid ^{1}H-NMR.[9] The β peak was implied to be weakly bound H species on Ru particles on the basis of the smaller heat of adsorption (10 kJ mol^{-1}) and larger H/Ru_{surf} ratio (3.3−5.6 at $P_{H_2} = 33-100$ kPa).

In this paper, we report the preparation of [Ru_6N] clusters on MgO, K^+/MgO, and Cs^+/MgO compared to that on Al_2O_3 as the first subject. The stability of [Ru_6C] clusters on MgO, La_2O_3, TiO_2, or Al_2O_3 was reported to be due to stabilization of the [Ru_6] framework by carbido carbon,[1,10] and similar stabilization was expected for supported [Ru_6N]. Detailed characterization of supported [Ru_6N] clusters was performed to determine (1) the homogeneity of supported [Ru_6N], (2) the kind of MgO surface sites where [Ru_6N] was attached, the (3) the nature of $Ru-O_{su}$ bonds (O_{su}, oxygen atom at surface), through the EXAFS observations for samples at different Ru wt % and the TPR (temperature-programmed reduction) measurements. Secondly, the reactivities of thus-characterized supported nitrido clusters with H_2 or N_2 were investigated by *in-situ* EXAFS measurements. These studies on the reactivity with H_2 and N_2 should be closely related with the catalysis (ammonia synthesis) on these nitrido clusters on a molecular level. The detailed discussions on the structures and their changes by the interaction with H_2 or N_2 are reported in this paper. The extension to catalysis is described in the accompanying paper.[11]

Experimental Section

$[PPN]^+[Ru_6N(CO)_{16}]^-$ (**1**) (PPN = $N(PPh_3)_2$)[12] ($[PPN]^+Cl^-$, Aldrich Chem Co., 97%; NaN_3, Wako Pure Chemical Ind., Ltd., >90%; $Ru_3(CO)_{12}$, Soekawa) was supported on MgO, K^+/MgO, Cs^+/MgO, or Al_2O_3 by reaction at 290 K (1 h) in purified THF (tetrahydrofuran, Wako, Special Grade) and the subsequent removal of THF in vacuum. The MgO (surface area 200 m^2 g^{-1}) was prepared from $Mg(OH)_2$ (Wako, 99.99%) by heating at 773 K (2 h) in vacuum. A water solution of Cs_2CO_3 (Wako, >95%) or K_2CO_3 (Wako, >99.5%) was impregnated on MgO, followed by treatments in O_2 and then in H_2 at 773 K. The Al_2O (aerosil C) (100 m^2 g^{-1}) was treated at 623 K (2 h) in vacuum. The loadings of Ru were 2.5 wt % for MgO, K^+/MgO, and Cs^+/MgO and 1.6 wt % for Al_2O_3 except for the EXAFS experiments at different Ru wt % for MgO (0.48, 2.5, and 3.9 wt %). The experiments at 0.48 and 3.9 wt % Ru were specified in the text, and those without special notation for MgO-supported samples were at 2.5 wt % Ru. The molar ratios $Cs^+/[Ru_6N]$ and $K^+/[Ru_6N]$ were fixed at 12 on the basis of the preliminary activity tests for ammonia synthesis. The supported nitrido−Ru clusters are denoted as [Ru_6N]/oxide.

$[PPN]^+_2[Ru_6(CO)_{18}]^{2-}$ (**2**) and $[NMe_3CH_2Ph]^+[Ru_6C(CO)_{16}Me]^-$ (**3**) ($[NMe_6CH_2Ph]^+Cl^-$, Wako; CH_3I, Wako, Special Grade) were supported on MgO in THF solution in a similar manner to the case of **1** or ref 1. The supported Ru clusters are denoted as [Ru_6]/MgO and [Ru_6C]/MgO (2.5 wt % Ru). The process of cluster catalyst preparation and transfer was carried out in argon (99.99%) or helium (99.99%). As pretreatment, incipient supported clusters were heated (elevating rate of temperature 4 K min^{-1}) in vacuum at 813 K except for $[Ru_6N]-Cs^+/MgO$ and $[Ru_6N]-K^+/MgO$ (heated at 673 K), followed by treatment in H_2 for 1 h (588−773 K).

The EXAFS spectra of the Ru K edge were measured for these supported clusters at the beamline 10B and 6B (2.5 GeV, current 360−260 A) of the Photon Factory in the National Laboratory for High Energy Physics (Proposal No. 93G010) between June 1993 and November 1994. The X-ray was monochronized through a double-crystal monochrometer of Si(311), and the spectra were obtained in the transmission mode with ionization chambers fitted with argon (I_0) and krypton (I). The energy resolution was ~1 eV at 9 keV, and the photon flux on the sample was $>10^9$/s. The sample was transferred to an EXAFS Pyrex cell ($0.13 < \Delta\mu t < 0.98$ dependent on the Ru wt %) with Kapton films on both sides by using the Schlenk technique from a closed circulating system for sample preparation. The data collection was performed at 30−293 K utilizing a closed cycle refrigerator (Cryo System, LTS-21). The analysis was performed by the program EXAFSH by Yokoyama et al.[13] The background subtraction was performed by calculating the cubic spline with three blocks, and the obtained function $\mu t(k) - \mu_0 t(k)$ was normalized by using the Victoreen parameter $\mu_0(\lambda) = C\lambda^3 - D\lambda^4$ to determine $\mu_0 t(k)$ and t. The Fourier transform (FT) of the k^3-weighted EXAFS oscillation was carried out over the range of $k_{min} = 3$ and $k_{max} = 13-16$ $Å^{-1}$ according to the signal/noise (S/N) of each spectrum. The window function (Hanning function) was multiplied with a k width of $(k_{max} - k_{min})/20$ on both ends of the FT k range. The inverse FT was performed in the r range of $r_{min} = 1.3-1.4$ and $r_{max} = 2.9-3.0$ Å multiplied by the window Hanning function with the width 0.1 Å on both ends. The curve-fitting analysis was performed by the method based on the formula of plane wave single-scattering theory,[14] using empirical phase shift and amplitude functions extracted from ruthenium powder for the Ru−Ru bond (metallic), RuO_2 for the Ru−O bond, $[RuCl_2(CO)_3]_2$ for the Ru(−C−)O bond, cluster **3** (Ru(−C−)Ru bond) for the Ru(−N−)Ru bond, and $Ru_3(CO)_{12}$ (Ru−C bond) for the Ru−C and Ru−N bonds (in the case of N_2 adsorbed on supported [Ru_6N] clusters). The parameters for the Ru−Ru bond (cluster) were obtained by subtracting the oscillation of the third shell of the complex $[RuCl_2(CO)_3]_2$ (Ru(−C−)O) from second shell of cluster **1** (Ru−Ru + Ru(−C−)O), taking into account each coordination number. The EXAFS spectra for these reference compounds were taken at room temperature. The residual factor (R_f) was calculated by the following equation:

$$R_f = \int |k^3\chi^{obs}(k) - k^3\chi^{calc}(k)|^2\, dk / \int |k^3\chi^{obs}(k)|^2\, dk$$

in the k region of 4−13 $Å^{-1}$ (4−12 for $[Ru_6N]-Cs^+/MgO$ in H_2 and 0.48 wt % [Ru_6N]/MgO because of their worse S/N) for the curve-fitting analysis. The H_2 (99.99%) and N_2 (99.99%) gas were purchased from Toyo Sanso Co., Ltd. The impurities (as molecular content) were less than the following values: $H_2O < 10$, $N_2 < 50$, $O_2 < 10$, $CO < 10$, $CO_2 < 10$ ppm and total hydrocabons < 10 ppm (as carbon content) in the H_2 gas, and $H_2O < 10$, $O_2 < 2$ ppm, and total hydrocarbons < 1 ppm (as carbon content) in the N_2 gas. The H_2 or N_2 was introduced to the EXAFS sample cell after further purification by passage through a liquid nitrogen trap.

FTIR spectra of supported nitrido clusters were recorded on a FTIR spectrometer (JASCO FTIR-5000) in a quartz IR cell

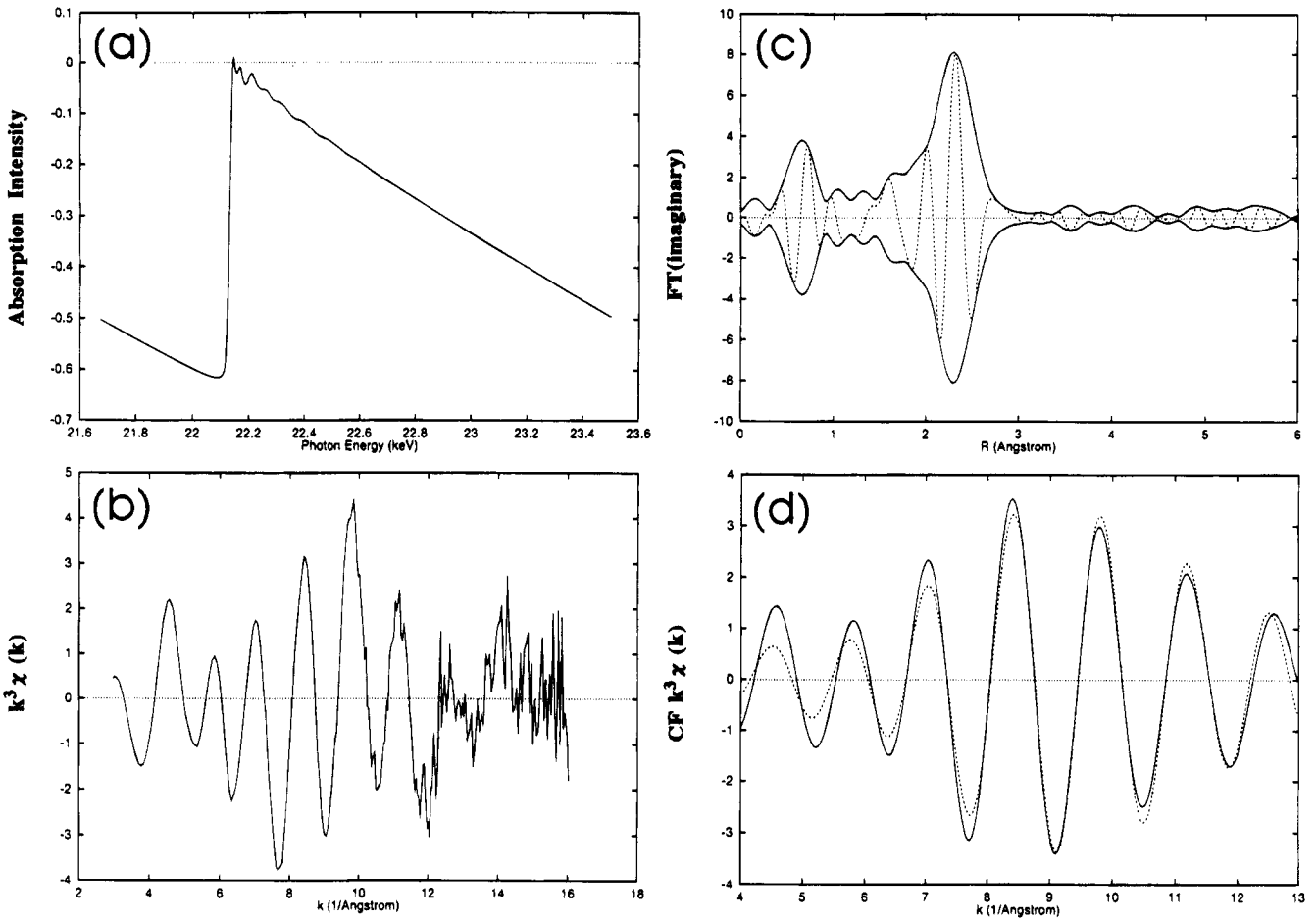

Figure 1. Ru K edge EXAFS spectra observed at 293 K for $[Ru_6N(CO)_{16}]^-$/MgO (2.5 wt % Ru). The sample was heated in vacuum (813 K) and in H_2 (588 K): (a) raw spectrum, (b) k^3-weighted EXAFS oscillation, (c) its associated Fourier transform, and (d) curve-fitting analysis, (—) observed, (- - -) calculated.

with NaCl windows on both sides combined with a closed circulating system. Support oxide disks were treated in the same conditions as powders in the IR cell and impregnated by a drop of a THF solution of cluster **1**. The temperature of the IR cell can be maintained at 295−823 K by a coil would around the cell.

Results

Characterization of Supported $[Ru_6N]$ Clusters on MgO, K^+/MgO, Cs^+/MgO, and Al_2O_3. *1. Incipient Supported Clusters.* The EXAFS spectra were observed for incipient $[Ru_6N]$/MgO, $[Ru_6N]-Cs^+$/MgO, and $[Ru_6N]/Al_2O_3$. The obtained coordination numbers N_{Ru-C} and $N_{Ru(-C-)O}$ were 2.5, 2.1, and 2.4−2.5, respectively, by the curve-fitting analysis. Corresponding numbers of carbonyl ligands per cluster would be 15, 13, and 14−15, respectively, in accordance with the total amount of desorbed CO + CO_2 in TPD (temperature-programmed desorption) measurements up to 813 K separately observed in vacuum (15, 12, and 16 on carbon basis). Although the incipient $[Ru_6N]$ framework was not affected upon supporting on MgO and Cs^+/MgO judging from the unchanged bonding distances r and N for Ru−Ru (first coordination) and Ru(−N−)Ru (diagonal line of octahedral (O_h) cluster $[Ru_6N]$) bondings, the Ru(−N−)Ru peak around 3.7 Å (phase shift uncorrected) disappeared in the FT of $k^3\chi$ for incipient $[Ru_6N]/Al_2O_3$ compared to the FT for unsupported cluster **1** (crystal). This suggested the distortion of the $[Ru_6N]$ framework (the angle $\theta_{Ru-N-Ru}$ was reduced from π)[15] by strong interaction with the Al_2O_3 surface.

2. Heated and Reduced Clusters. The incipient $[Ru_6N]$/MgO and $[Ru_6N]/Al_2O_3$ were heated in vacuum at 813 K (up to the temperature where CO ligands had totally desorbed) and then in H_2 at 588 K. The obtained EXAFS spectra were almost identical after heating and after subsequent H_2 treatment for $[Ru_6N]$/MgO (Figure 1a,b). Also, the corresponding two spectra were almost identical for $[Ru_6N]/Al_2O_3$. Therefore, common ruthenium cluster species were suggested for samples with/without the H_2 treatment at 588 K. The EXAFS spectrum for $[Ru_6N]$/MgO after heating and in H_2 is shown in Figure 1. A strong peak ascribable to Ru−Ru bonding and a shoulder on the shorter distance side of the Ru−Ru peak were observed (Figure 1c). By the curve-fitting analysis with two waves (Ru−Ru, Ru−O), the coordination number of Ru−Ru bonding (N_{Ru-Ru}) was calculated to be 4.1 with r_{Ru-Ru} = 2.62 Å (Table 1 and Figure 1d), similar to the value for cluster **1** (=4), indicating that the $[Ru_6N]$ unit remained on MgO in H_2 at 588 K. An alternative curve-fitting analysis was performed with one wave (Ru−Ru) or three waves (Ru−Ru, two Ru−O), and the R_f values were 6.8 and 2.8%, respectively. In the one-wave fitting (Ru−Ru), the calculated curve did not trace the inversely Fourier-transformed experimental curve in all wavenumber regions. In the three-wave fitting (Ru−Ru, two Ru−O), the fitting was not improved by the addition of one more Ru−O wave to two waves (Ru−Ru, Ru−O). Thus, the analysis with two waves (Ru−Ru, Ru−O) was reasonable with smaller R_f: 2.5% (Table 1). The obtained $N_{Ru-O_{su}}$ (0.5) suggests that one triangle Ru_3 face of the O_h-like $[Ru_6N]$ framework was attached on the MgO surface through three $Ru-O_{su}$ bonds. If the O_h-like structure was destroyed to a raftlike structure by the

TABLE 1: Results for the Curve-Fitting Analysis of Ru K Edge EXAFS (Observed at 293 K) for Supported $[Ru_6N(CO)_{16}]^-$ Clusters on MgO, K^+/MgO, Cs^+/MgO, and Al_2O_3 after Heating in Vacuum (813[a] or 673 K[b]) and in Hydrogen (588 K)[c]

		Ru−Ru				Ru−O				
support	Ru wt %	N	r[d]	ΔE_0[e]	$\Delta(\sigma^2)$[f]	N	r	ΔE_0	$\Delta(\sigma^2)$	R_f
MgO[a]	2.5	4.1	2.62	−7.4	4.0	0.5	2.13	12	−2.2	2.5
K^+/MgO[b]	2.5	3.8	2.63	−14	3.7	0.6	2.00	−13	0.87	5.2
Cs^+/MgO[b]	2.5	4.0 (±0.6)	2.63 (±0.016)	−13 (±4)	3.6 (±1.2)	0.6 (±0.2)	2.03 (±0.027)	−4.1 (±2.7)	0.94 (±0.67)	3.2 (±1.6)
Al_2O_3[a]	1.6	2.0	2.61	−8.9	0.49	1.9	2.16	1.7	1.9	0.6

[a] MgO and Al_2O_3 catalysts heated at 813 K. [b] K^+/MgO and Cs^+/MgO catalysts heated at 673 K. [c] K^+ (*or* Cs^+)/[Ru_6N] = 12 in mol ratio. The error (within the 50% increase of R_f) is shown in parentheses. [d] In Å (Å = 10^{-1} nm). [e] In eV. [f] In 10^{-3} Å^2.

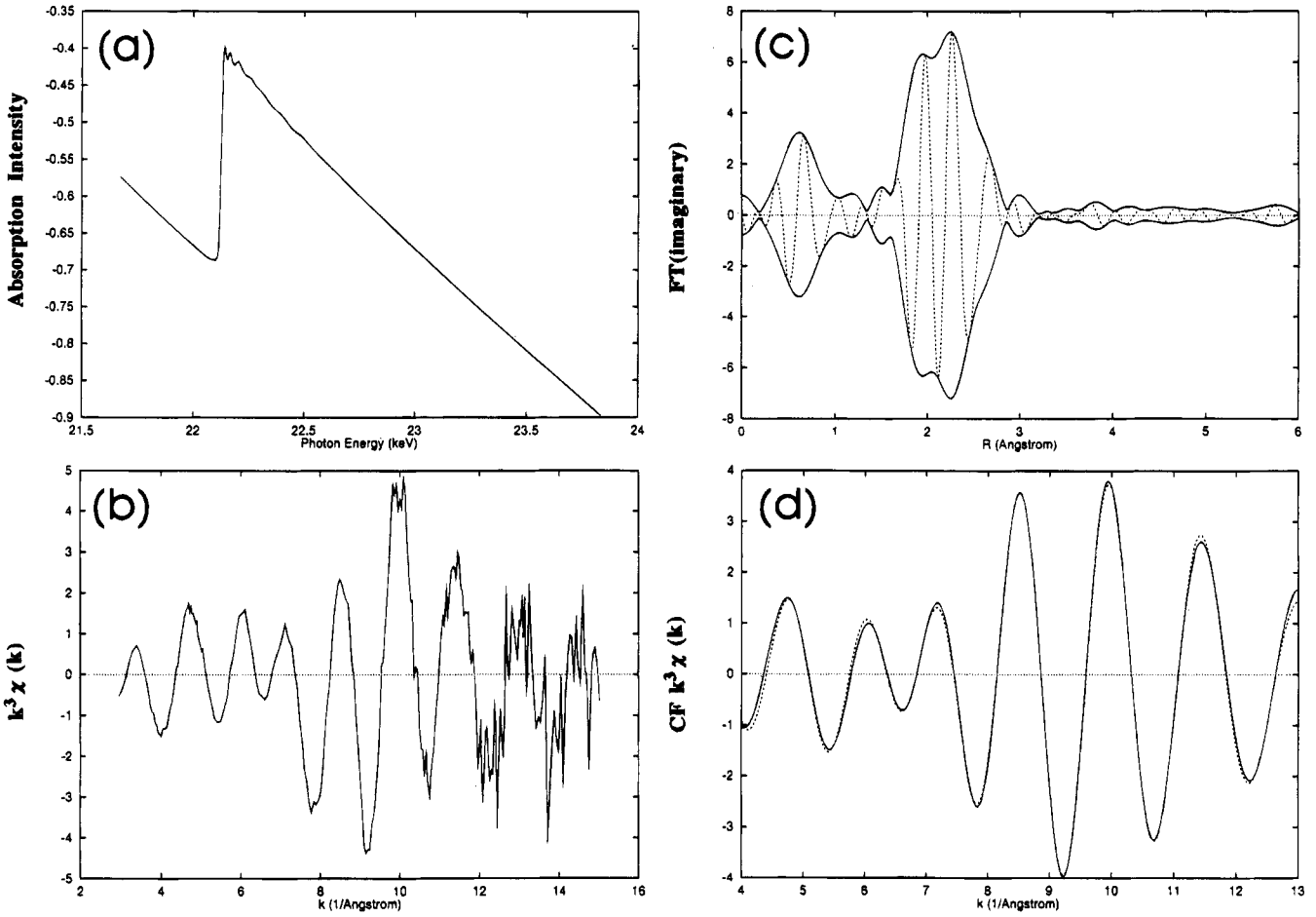

Figure 2. Ru K edge EXAFS spectra observed at 293 K for $[Ru_6N(CO)_{16}]^-/Al_2O_3$ (1.6 wt % Ru). The sample was heated in vacuum (813 K) and in H_2 (588 K). The captions for (a)−(d) are the same as in Figure 1.

interaction with the MgO surface, N_{Ru-Ru} should be smaller than the observed 4.1. Hence, we suppose the formulation [Ru_6N-(μ-O_{su})$_3$] ($N_{Ru-O_{su}}$ = 2.13 Å). The cluster **1** was suggested to interact with the Al_2O_3 surface and be distorted to lose O_h symmetry of the [Ru_6N] framework, as indicated by the disappearance of Ru(−N−)Ru bonding for the incipient cluster (in the previous section). The EXAFS spectra for [Ru_6N]/Al_2O_3 after heating and in H_2 are shown in Figure 2, and curve-fitting result is listed in Table 1. The N_{Ru-Ru} decreased to 2.0, and $N_{Ru-O_{su}}$ was 1.9. The formation of the trimer [$Ru_3(\mu_2$-$O_{su})_3$] cluster was suggested after the fragmentation from hexamer nitrido cluster **1** by strong interaction with the Al_2O_3 surface. The coordination of O_{su} should be μ_2 (coordinate to two Ru atoms) in order to be consistent with $N_{Ru-O_{su}}$ (1.9) taking into account the [Ru_3] cluster size and the population of O_{su} at the Al_2O_3 surface (see the Discussion section).

Also, [Ru_6N]−K^+/MgO and [Ru_6N]−Cs^+/MgO heated in vacuum at 673 K showed very little change of EXAFS spectra by subsequent H_2 treatment at 588 K. The EXAFS spectra are shown in Figure 3 for [Ru_6N]−Cs^+/MgO heated in vacuum at 673 K and in H_2 at 588 K. Corresponding curve-fitting results are listed in Table 1. The result was similar to that for [Ru_6N]/MgO, and N_{Ru-Ru} of 3.8 on K^+/MgO and 4.0 on Cs^+/MgO suggest retention of the [Ru_6N] unit on K^+/MgO and Cs^+/MgO. However, the $r_{Ru-O_{su}}$ values were 2.00−2.03 Å for [Ru_6N]−K^+/MgO and [Ru_6N]−Cs^+/MgO, which were shorter by 0.10−0.13 Å than that for [Ru_6N]/MgO (2.13 Å) (Table 1).

3. The Change of [Ru_6N] Cluster Structure and MgO Sites at Different Ru wt %. The EXAFS spectra were also measured for [Ru_6N]/MgO at 0.48 and 3.9 wt % Ru. The EXAFS spectrum of a sample at 0.48 wt % Ru is shown in Figure 4. Compared to the Fourier transform for the 2.5 wt % Ru sample (Figure 1c), the peak around 1.7 Å (Ru−O) (phase shift uncorrected) became stronger, while the peak around 2.3 Å did not show significant change (Figure 4c). The best fit result is listed in Table 2 and shown in Figure 4d. The N_{Ru-Ru} (4.0) suggested that the [Ru_6N] cluster unit was retained also at 0.48 wt % Ru on the MgO surface.

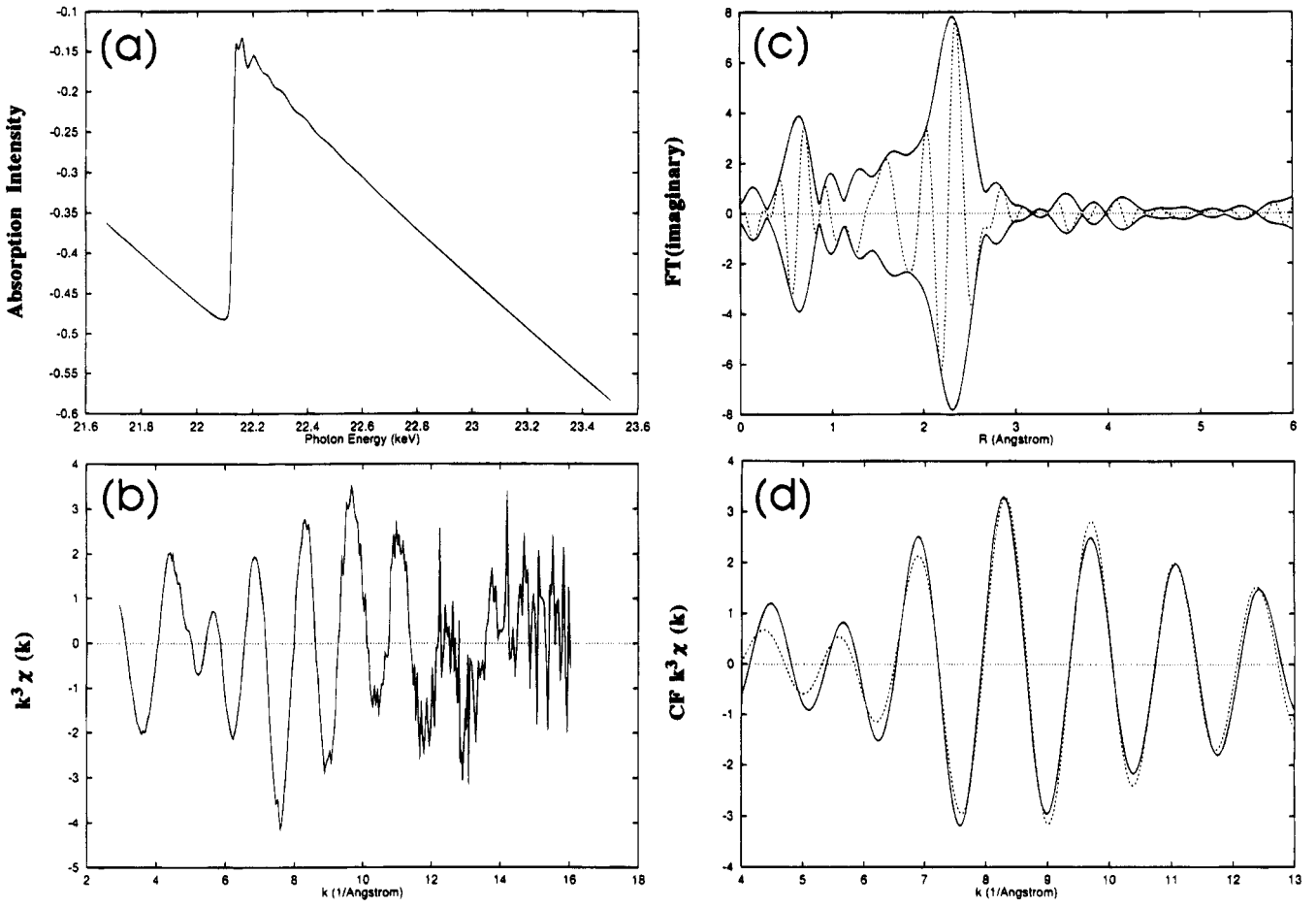

Figure 3. Ru K edge EXAFS spectra observed at 293 K for $[Ru_6N(CO)_{16}]^-$−Cs^+/MgO (2.5 wt % Ru, $Cs^+/[Ru_6N]$ = 12 in mol ratio). The sample was heated in vacuum (673 K) and in H_2 (588 K). The captions for (a)−(d) are the same as in Figure 1.

The N_{Ru-Ru} for $[Ru_6N]$/MgO at 3.9 wt % Ru was 5.0 with the same r_{Ru-Ru} (2.62 Å) as for the sample at 2.5 wt % Ru (Table 2). The $[Ru_6N]$ clusters should have aggregated to larger Ru particles similar to $[Ru_6N]$/MgO (2.5 wt % Ru) in H_2 at 653−773 K (N_{Ru-Ru} = 4.9−6.6, EXAFS). The surface cluster species $[Ru_6N]$ were stable in H_2 or in reaction conditions of $N_2 + H_2$, but aggregated to larger metal particles in more severe conditions or with larger Ru loadings (Ru ~ 4 wt %). The N_{Ru-Ru} of $[Ru_6]$/MgO (without interstitial atom) prepared from non-nitrido cluster **2** was 5.9 in vacuum at 813 K and 6.2 in H_2 at 588 K by EXAFS, indicating the aggregation of the $[Ru_6]$ cluster to larger particles in vacuum at 813 K and/or in H_2 at 588 K in the case of cluster **2** (without nitrido N).

4. TPR Measurements for $[Ru_6N]$/MgO, $[Ru_6N]$−Cs^+/MgO, and $[Ru_6]$/MgO. We studied TPR in H_2 by mass spectroscopy for incipient $[Ru_6N]$/MgO, $[Ru_6N]$−Cs^+/MgO, and $[Ru_6]$/MgO (Figure 5a). These spectra had common peaks of NH_3 around 510 K, but higher temperature peaks of NH_3 were observed around 660 K only for $[Ru_6N]$/MgO and $[Ru_6N]$−Cs^+/MgO. As the former desorption temperature (around 510 K) coincided with the disappearing temperature of the IR peak of $[PPN]^+$ (cation of clusters **1** and **2**) (1117 cm^{-1}) (Figure 5b), we believe that the peaks around 660 K originated from nitrido N of **1**. This TPR result supported the structure $[Ru_6N(\mu\text{-}O_{su})_3]$ on MgO, K^+/MgO, and Cs^+/MgO.

The Reactivity of Supported $[Ru_6N]$ Clusters on MgO and Cs^+/MgO with H_2/N_2. *1. With H_2.* The FT of the EXAFS at 193 K for $[Ru_6N(\mu\text{-}O_{su})_3]$ on MgO in H_2 (76 kPa) slightly shifted to the longer distance side compared to those in vacuum (Figure 1), and the obtained curve-fitting data indicated the change of bond distance of r_{Ru-Ru} from 2.62 to 2.65 Å with the change of $r_{Ru-O_{su}}$ from 2.13 to 2.17 Å by the adsorption of H_2 (Table 3). The sample after evacuation of H_2 at 193 K was very similar to the EXAFS of the initial supported cluster before H_2 introduction (Figure 1), suggesting that this structure change by the hydrogen adsorption/desorption was reversible. The control EXAFS experiment was carried out for $[Ru_6N]$/MgO in vacuum at 30−193 K. The obtained r_{Ru-Ru} (2.62 Å) at 30 K) in Table 3 was the same as that for $[Ru_6N]$/MgO in vacuum at 293 K (Table 1), excluding the possibility of the expansion/contraction of the $[Ru_6N]$ cluster framework by cooling/heating.

The reactivity of $[Ru_6N]$−Cs^+/MgO with H_2 (76 kPa) was also examined by EXAFS. Compared to $k^3\chi$ observed in vacuum (Figure 3b), we observed a drastic change of EXAFS in H_2 (Figure 6b). In its associated FT (Figure 6c), the bonding distance of the main peak (Ru−Ru) became larger (phase shift uncorrected) than those in vacuum (Figure 3). The r_{Ru-Ru} obtained by curve fitting (Figure 6d) was 2.71 Å for the sample in H_2 (Table 3), longer by 0.08 Å than for the sample in vacuum (2.63 Å, Table 1). Additional analyses were performed by changing the FT range, CF range, N, or r, independently, and also for another EXAFS spectrum of the same sample in the same conditions in order to estimate the errors. The errors for r_{Ru-Ru} were ±0.016 and ±0.015 Å for spectra corresponding to Figures 3 and 6 (Table 1 and 3). Therefore, it is valid to think that the r_{Ru-Ru} change (±0.08 Å) was induced by hydrogen expansion/contraction.

As a reference, incipient $[Ru_6C]$/MgO was heated in vacuum and in H_2 at 623 K. The non-nitrido Ru hexamer cluster $[Ru_6(\mu\text{-}O_{su})_x]$ was suggested to be formed from the equimolar desorption data for CH_4[1] and the EXAFS data r_{Ru-Ru} (2.63 Å) and N_{Ru-Ru} (4.2) (Table 4). The number x should be 3−4

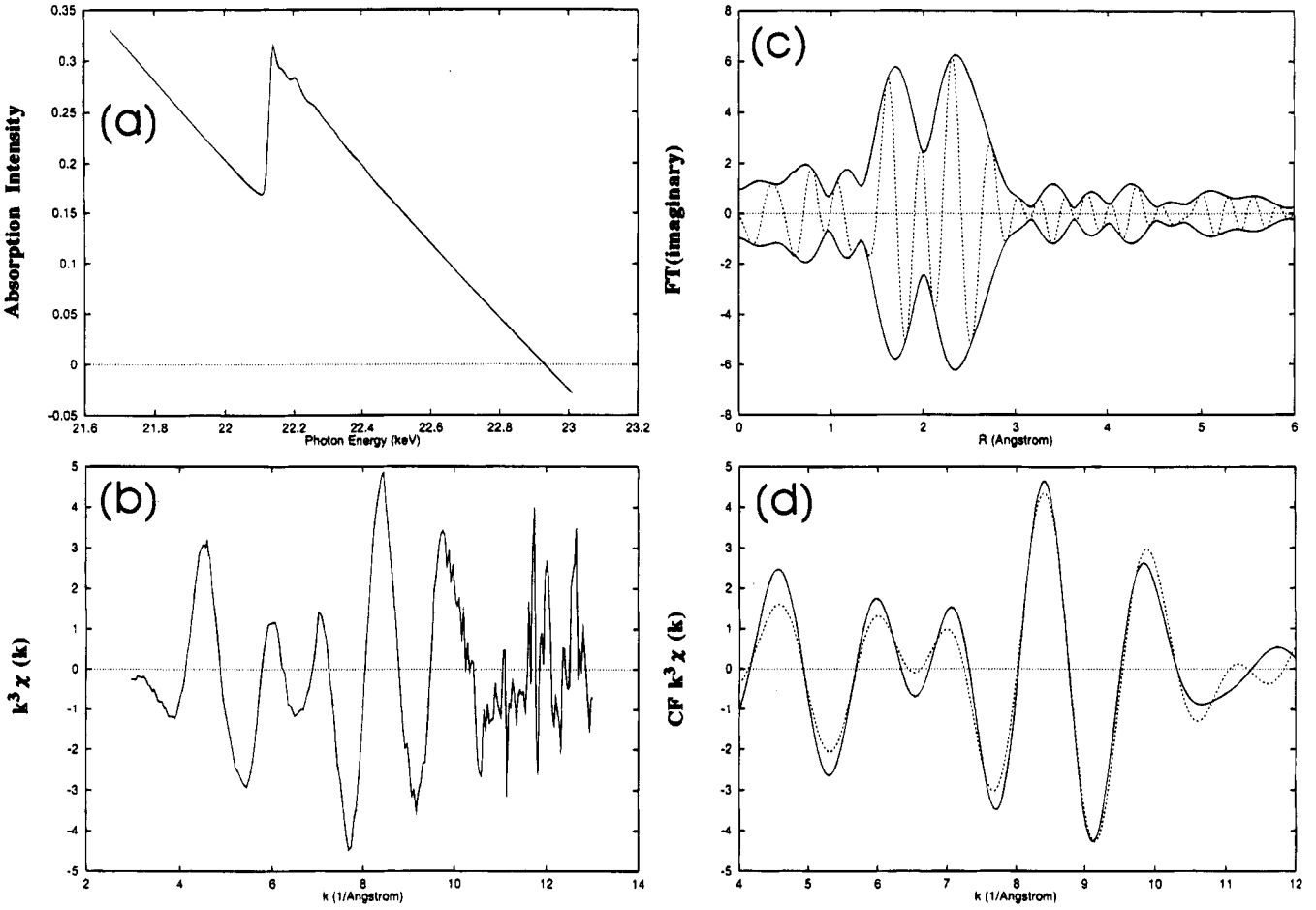

Figure 4. Ru K edge EXAFS spectra observed at 293 K for $[Ru_6N(CO)_{16}]^-$/MgO (0.48 wt % Ru). The sample was heated in vacuum (813 K) and in H_2 (588 K). The captions for (a)−(d) are the same as in Figure 1.

TABLE 2: Results for the Curve-Fitting Analysis of Ru K Edge EXAFS (Observed at 293 K) for $[Ru_6N(CO)_{16}]^-$/MgO at Different Ru wt % (0.48, 2.5, and 3.9 wt %)[a]

	Ru−Ru				Ru−O				
Ru wt %	N	r^b	$\Delta E_0{}^c$	$\Delta(\sigma^2)^d$	N	r	ΔE_0	$\Delta(\sigma^2)$	R_f
0.48	4.0	2.65	−0.4	4.6	1.2	2.09	4.1	−3.0	4.8
2.5	4.1	2.62	−7.4	4.0	0.5	2.13	12	−2.2	2.5
3.9	5.0	2.62	−9.4	3.5	0.3	2.20	13	−5.0	4.7

[a] The samples were treated in the same conditions as in table 1. [b] In Å. [c] In eV. [d] In 10^{-3} Å^2.

judging from $N_{Ru-O_{su}}$ (0.6). In H_2, the cluster showed no structural change of cluster framework (Table 4).

2. With N_2. The EXAFS spectrum was observed for [Ru_6N-(μ-O_{su})$_3$] on MgO in N_2 (25 kPa) at 193 K. In its FT, a shoulder peak on the lower distance side than Ru−Ru bonding became stronger than in Figure 1c. The data were best fitted with three waves, Ru−Ru, Ru−O_{su}, and Ru−N, with the distances 2.62, 2.13, and 1.95 Å (R_f 1.7%, in Table 3) rather than two waves (Ru−Ru, Ru−O_{su}) (R_f 4.0%). The N_{Ru-N} (0.4) by three-wave fitting suggested two or three on-top N_2(a) or one or two bridging N_2(a) on the Ru cluster because molecular N_2 should not be dissociated at 193 K. The N and r for Ru−Ru and Ru−O_{su} bondings did not change by the adsorption of N_2 (N_{Ru-Ru} = 4.1 ± 0.1, r_{Ru-Ru} = 2.62 Å, $N_{Ru-O_{su}}$ = 0.5, $r_{Ru-O_{su}}$ = 2.13 Å (Tables 1 and 3).

. The interaction with N_2 (25 kPa) was also examined for [Ru_6N]−Cs^+/MgO. The curve-fitting analysis with three waves, Ru−Ru, Ru−O_{su}, and Ru−N, improved the fitting compared to two-wave (Ru−Ru, Ru−O_{su}) fitting, especially in the lower k region. The obtained r for Ru−Ru and Ru−O_{su} bondings by three-wave fitting (Table 3) showed slight changes (Δr_{Ru-Ru} = 0.02 Å, $\Delta r_{Ru-O_{su}}$ = 0.04 Å) compared to the sample in vacuum (Table 1). The r_{Ru-N} was 2.02 Å, larger by 0.07 Å than for N_2(a) on [Ru_6N]MgO (Table 3).

Discussion

Cluster Structures. The $[Ru_6N(CO)_{16}]^-$ cluster **1** interacted with MgO to form $[Ru_6N(CO)_{16-x}]^{n-}$ ($x \sim 1$), releasing one CO at room temperature, and transformed to [Ru_6N(μ-O_{su})$_3$] (Figure 7) by the decarbonylation in vacuum at 813 K (Figure 1 and Table 1). The attached cluster framework structure did not change by subsequent treatment in H_2 at 588 K or the treatment in N_2 and H_2 at 588 K (r_{Ru-Ru} = 2.62 Å, $r_{Ru-O_{su}}$ = 2.13 Å). On Cs^+-doped MgO and K^+-doped MgO, the cluster **1** interacted with Cs^+/MgO or K^+/MgO to form [Ru_6N-$(CO)_{16-x}]^{m-}$ ($x \sim$ 3-4), releasing three to four CO ligands from the cluster, and transformed to [Ru_6N(μ-O_{su})$_3$] (Figure 7) by the evacuation at 673 K and hydrogen treatment at 588 K (r_{Ru-ru} = 2.63 Å, $r_{Ru-O_{su}}$ = 2.03 Å on Cs^+/MgO and r_{Ru-Ru} = 2.63 Å, $r_{Ru-O_{su}}$ = 2.00 Å on K^+/MgO, in Table 1). In contrast, cluster **1** transformed to [Ru_3(μ_2-O_{su})$_3$] on Al_2O_3 by the evacuation at 813 K (Figure 7), and the species were very stable in H_2 at 588−773 K (Table 1). This triangle cluster (r_{Ru-Ru} = 2.61 Å, $r_{Ru-O_{su}}$ = 2.16 Å) should be similar to [Ru_3(μ_2-O_{su})$_3$] on Al_2O_3 prepared from cluster **2** ($r_{Ru-O_{su}}$) = 2.06 Å).[1] Considering the crystal structures of Al_2O_3 (corundum for α and spinal for γ) and MgO (NaCl-type), the smallest interatomic distances of two O_{su} atoms at 2.8 Å for Al_2O_3 and 2.98 Å for MgO. Compared to the r_{Ru-Ru} of attached Ru clusters (2.61 Å for Al_2O_3 and 2.62 Å for MgO, Table 1), the obtained $N_{Ru-O_{su}}$ (1.9) for [Ru_3] species on Al_2O_3 can be interpreted only as the μ_2 coordination

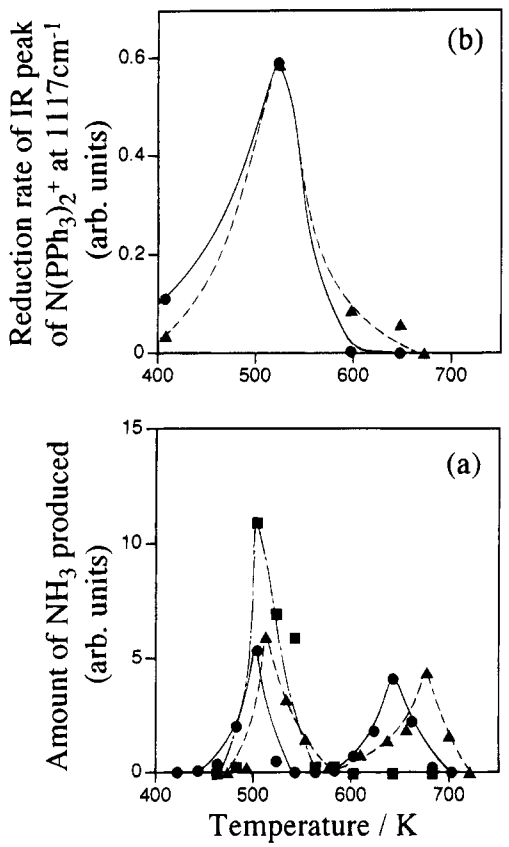

Figure 5. Temperature-programmed reduction (TPR) in H_2 for incipient $[Ru_6N(CO)_{16}]^-$/MgO (●), $[Ru_6N(CO)_{16}]^-$–Cs^+/MgO (▲), and $[Ru_6(CO)_{18}]^{2-}$/MgO (■): (a) NH_3 desorption monitored by mass; (b) the decrease rate of the IR peak at 1117 cm^{-1}. The heating rate is 4 K min^{-1}.

of three O_{su} atoms. The $N_{Ru-O_{su}}$ (0.5) for $[Ru_6N]$ species on MgO can be understood as three O_{su} atoms coordinated to one triangle face $[Ru_3]$ of the O_h-like $[Ru_6N]$ species as the μ_1 coordination. This coordination style of $[Ru_6N]$ species on MgO was ensured by the Ru wt % dependence of $N_{Ru-O_{su}}$ (see below). The other examples of metal–O_{su} bond distances (2.00–2.83 Å) were summarized in ref 2 for the supported Ru, Rh, Pd, Re, Os, Ir, or Pt clusters, and the distances were classified as either in the range 2.00–2.24 Å or in the range 2.63–2.83 Å. Observed $r_{Ru-O_{su}}$ values for $[Ru_6N(\mu\text{-}O_{su})_3]$ on MgO (2.13 Å), K^+/MgO (2.00 Å), Cs^+/MgO (2.03 Å), or Al_2O_3 (2.16 Å) were within the range 2.00–2.24 Å, similar to other supported Ru, Rh, Re, or Os clusters. In the curve-fitting analyses in Tables 1–3 for N_2-free samples, all the Fourier-filtered $k^3\chi$ were well fitted with two waves (Ru–Ru, Ru–O_{su}). The addition of a Ru–N_{int} (N_{int}, interstitial nitrogen) wave (2.06 Å) was needed to fit the EXAFS of cluster **1** (powder) as the bonding between Ru and N_{int}. The reason that the additional wave was not needed to fit the experimental data in Tables 1–3 may be electron donation from N_{int} to $[Ru_6]$, as suggested by IR and the distorted framework structure of $[Ru_6N]$ from its O_h symmetry when unsupported.[15] Similarly, Ru K edge EXAFS for supported $[Ru_6C]$ was well fitted without a Ru–C_{int} wave probably due to the chemical state of C_{int} (with less electrons) as a backscattering atom in EXAFS and the distortion of the $[Ru_6C]$ framework.[1,2]

The dependence of cluster structure on Ru wt % was examined for $[Ru_6N]$/MgO at 0.48, 2.5, and 3.9 wt % Ru. On the basis of the surface area of MgO (200 m^2 g^{-1}), r_{Mg-O} (2.106 Å), and the number of surface OH groups of MgO heated at 773 K (~5 nm^{-2}),[16] the numbers of surface O atom (O_{su}) and surface OH groups were estimated to be 2.3×10^{21} and 1×10^{21} per gram of MgO, respectively. On MgO, OH groups were observed as a sharp strong peak at 3757 cm^{-1} in addition to a weaker broad peak around 3614 cm^{-1} after pretreatment at 773 K, and the peak intensity of these peaks did not change by the interaction with cluster **1** in THF and/or heating in vacuum at 813 K. The number of attached $[Ru_6N]$ clusters was 4.8×10^{18}, 2.4×10^{19}, and 4.0×10^{19} per gram of MgO in the case of 0.48, 2.5, and 3.9 wt % Ru samples, respectively. It was difficult to monitor the MgO surface sites which were reacted with $[Ru_6N]$ clusters because the reaction of incipient $[Ru_6N(CO)_{16-x}]^{n-}$ (partially decarbonylated) with the MgO surface (to form Ru–O_{su} bondings) occurred during heating in vacuum (813 K), accompanying the total decarbonylation. However, the number of surface OH groups was larger by about 30 times than that of $[Ru_6N]$ for the 3.9 wt % Ru sample, and the $N_{Ru-O_{su}}$ changed very critically with different Ru loadings (Table 2). In this context, we believe the reaction of the cluster is with O_{su}, *not* with *OH*. As the (001) face is believed to be predominantly exposed for MgO even as a powder,[17] two models of supported $[Ru_6N(\mu\text{-}O_{su})_x]$ were proposed on major sites of MgO(001) (Figure 8a) and on fewer sites on MgO(001) with steps (Figure 8b). We think that the $[Ru_6N]$ with low Ru loading (Ru ~ 0.5 wt %) mainly interacted with the lower coordination MgO surface to form $[Ru_6N(\mu\text{-}O_{su})_x]$ ($x = 5-7$), such as in Figure 8b ($N_{Ru-O_{su}} = 0.83$ as a model), on the basis of the obtained $N_{Ru-O_{su}}$ by EXAFS (1.2, Table 2). The $[Ru_6N]$ at moderate Ru loading (Ru ~ 2.5 wt %) mainly interacted with relatively flat MgO planes to form $[Ru_6N(\mu\text{-}O_{su})_3]$, similar to Figure 8a ($N_{Ru-O_{su}} = 0.5$ as a model), on the basis of the obtained $N_{Ru-O_{su}}$ by EXAFS (0.5, Table 2). Heterolytic fragmentations of $[Ru_6N]$ by heating in vacuum at 813 K, such as from $[Ru_6N]$ to $[Ru_5N]$ + Ru, seemed improbable on the basis of wavenumbers and the peak pattern of adsorbed CO (in IR) on $[Ru_6N]$/MgO (heated at 813 K and in H_2 at 588 K) at 0.06 wt % Ru (1978w(sh), 1965s) similar to that at 2.5 wt % (2059w(sh), 2045w(sh), 1992s),[11] without specific twin or triple peaks ascribable to surface $Ru(CO)_x$ species.[18–20]

The nuclearity of $[Ru_6N]$ on MgO, Cs^+/MgO, or K^+/MgO did not change by heating in vacuum or in H_2 probably due to the strong binding of $[Ru_6]$ by nitrido nitrogen on the basis of the experimental facts of the retention of nitrido N below ~600 K in H_2 in TPR (Figure 5a) and the N_{Ru-Ru} (about 4) by EXAFS (Tables 1–3). The 100%-raft $[Ru_6]$ on flat MgO(001) cannot explain the observed $N_{Ru-O_{su}} = 1.2$ ($r_{Ru-O_{su}} = 2.09$ Å) with $N_{Ru-Ru} = 4.0$ ($r_{Ru-Ru} = 2.65$ Å) at 0.48 wt % Ru (Table 2) because the N_{Ru-Ru} should be around 3 for raft $[Ru_6]$. We believe the selective reaction of O_h-$[Ru_6N]$ with a lower coordination MgO surface at lower Ru loadings was quite probable due to higher reactivity of lower coordination surface sites. The $r_{metal-O_{su}}$ distances were 2.09–2.17 Å for $[Ru_6N]$/MgO (Tables 2 and 3), 2.00 Å for $[Ru_6N]$–K^+/MgO (Table 1), and 2.03–2.07 Å for $[Ru_6N]$–Cs^+/MgO (Tables 1 and 3). The $r_{Ru-O_{su}}$ distances were shorter on K^+- or Cs^+-doped MgO (2.00–2.03 Å) than on alkali-undoped MgO (2.13 Å) after the incipient clusters were heated at 813 or 673 K (Table 1). The distances $r_{Ru-O_{su}}$ for $[Ru_6N]$/MgO were always longer (2.09–2.20 Å) than $[Ru_6N]$–A^+/MgO (A = K, Cs) (2.00–2.07 Å) at any Ru wt % and in H_2 or N_2 (Tables 1–3), implying the $[Ru_6N(\mu\text{-}O_{su})_3]$ clusters were coordinated to O_{su} bonded to K^+ or Cs^+ ions on K^+/MgO or Cs^+/MgO (Figure 7).

Similar to the supported nitrido $[Ru_6N]$ clusters, the carbido clusters **3** transferred to $[Ru_6C(\mu\text{-}O_{su})_3]$ ($r_{Ru-Ru} = 2.63$ Å, $r_{Ru-O_{su}} = 2.12$ Å) on MgO by heating in vacuum at 623 K.[1,2] By further treatment in H_2 at 623 K, it lost carbido carbon and was

TABLE 3: Results for the Curve-Fitting Analysis of Ru K Edge EXAFS (Observed at 193,[a] 100,[b] and 30 K[c]) for $[Ru_6N(CO)_{16}]^-$/MgO and $[Ru_6N(CO)_{16}]^-$-Cs^+/MgO in H_2 or N_2[d]

		Ru−Ru				Ru−O				Ru−N				
support	gas	N	r[e]	ΔE_0[f]	$\Delta(\sigma^2)$[g]	N	r	ΔE_0	$\Delta(\sigma^2)$	N	r	ΔE_0	$\Delta(\sigma^2)$	R_f
MgO	vacuum[c]	3.9	2.62	−11	0.36	0.7	2.15	7.0	−0.05					4.9
	H_2[a]	4.2	2.65	−7.9	3.6	0.5	2.17	5.2	−1.5					2.3
	N_2[a]	4.2	2.62	−9.9	3.0	0.5	2.13	6.8	−3.9	0.4	1.95	−13	10	1.7
Cs^+/MgO	H_2[b]	4.0 (±0.5)	2.71 (±0.015)	−14 (±5)	3.5 (±0.6)	0.6 (±0.2)	2.06 (±0.010)	1.2 (±1.1)	−2.1 (±2.2)					3.8 (±1.9)
	N_2[a]	3.7	2.65	−6.9	5.8	0.7	2.07	6.4	−3.0	0.7	2.02	8.9	4.3	1.9

[a] MgO catalyst in H_2 and N_2 and Cs^+/MgO catalyst in N_2 observed at 193 K. [b] Cs^+/MgO catalyst in H_2 observed at 100 K. [c] MgO catalyst in vacuum observed at 30 K. [d] The samples were treated in the same conditions as Table 1. The error (within the 50% increase of R_f) is shown in parentheses. [e] In Å. [f] In eV. [g] In 10^{-3} Å^2.

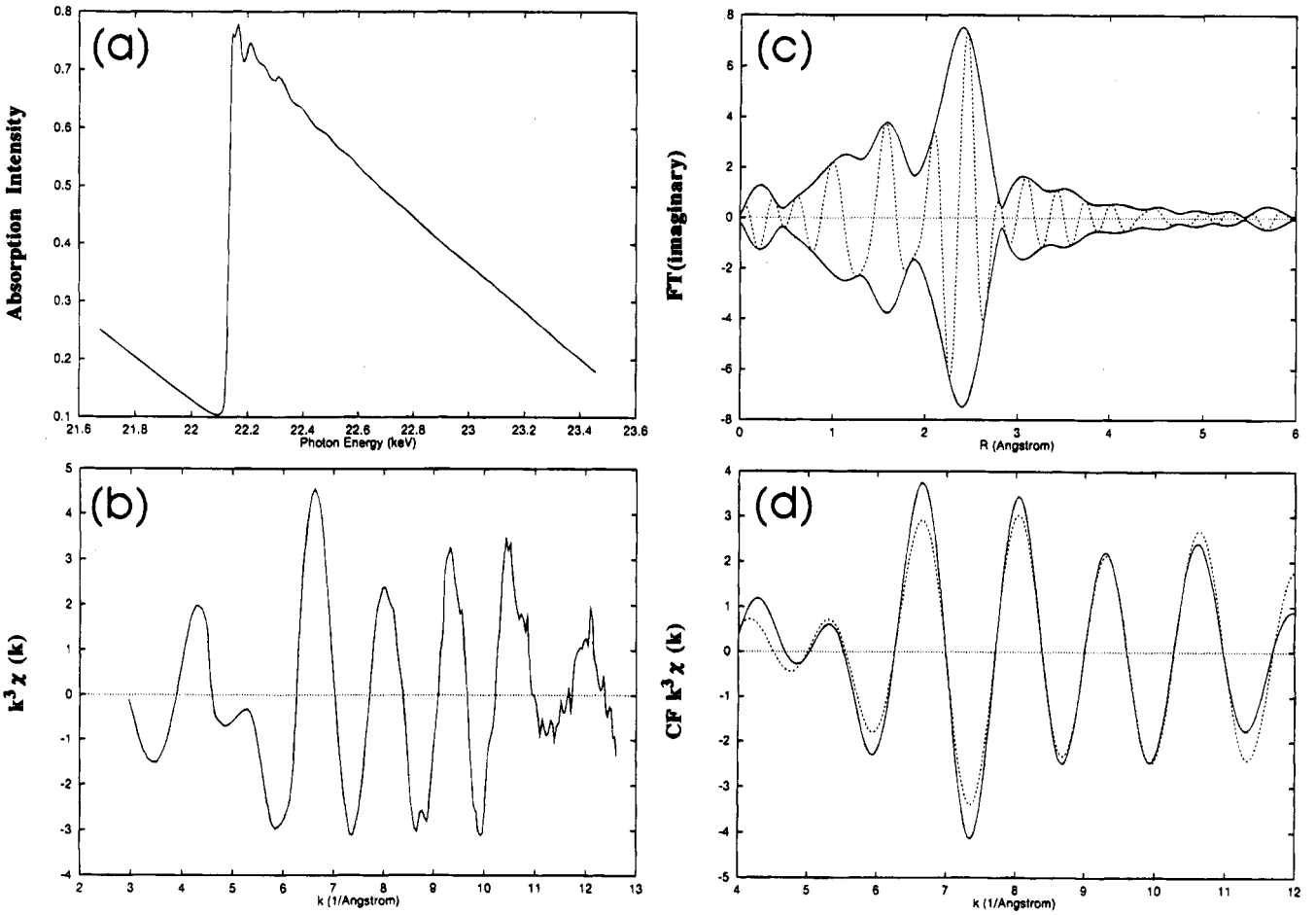

Figure 6. Ru K edge EXAFS spectra observed at 100 K for $[Ru_6N(CO)_{16}]^-$−Cs^+/MgO (2.5 wt % Ru, $Cs^+/[Ru_6N]$ = 12) in H_2 (76 kPa). The sample was heated in vacuum (673 K) and in H_2 (588 K). The captions for (a)−(d) are the same as in Figure 1.

TABLE 4: Results for the Curve-Fitting Analysis of Ru K Edge EXAFS (Observed at 293[a] and 100 K[b]) for $[Ru_6(\mu\text{-}O_{su})_{3-4}]$ on MgO Prepared from $[Ru_6C(CO)_{16}Me]^-$ in Vacuum and in H_2 at 623 K[c]

	Ru−Ru				Ru−O				
gas	N	r[d]	ΔE_0[e]	$\Delta(\sigma^2)$[f]	N	r	ΔE_0	$\Delta(\sigma^2)$	R_f
vacuum[a]	4.2	2.63	−10	2.2	0.6	2.10	0.7	−0.3	4.2
H_2[b]	3.7	2.63	−7.9	1.5	0.7	2.11	2.3	−0.5	3.3

[a] In vacuum at 293 K. [b] In H_2 at 100 K. [c] The samples were treated in the same conditions as in Table 1. [d] In Å. [e] In eV. [f] In 10^{-3} Å^2.

transformed to $[Ru_6(\mu\text{-}O_{su})_{3-4}]$ (r_{Ru-Ru} = 2.63 Å, $r_{Ru-O_{su}}$ = 2.10 Å) on MgO (Table 4). Corresponding TPR in H_2 for $[Ru_6C]$/MgO had a peak of CH_4 around 560 K (carbido C desorbed as CH_4),[1] similar to the peak of NH_3 around 660 K for $[Ru_6N]$/MgO and $[Ru_6N]$−Cs^+/MgO (Figure 5a). The cluster **2** without an interstitial atom readily aggregated to larger Ru particles on MgO during the evacuation at 813 K and/or subsequent H_2 treatment at 588 K (N_{Ru-Ru} = 5.9−6.2). Thus, nitrido N (or carbido C) was suggested to maintain the $[Ru_6]$ cluster framework by binding from the inside even at high temperatures or in H_2.

Cluster Structure Changes in H_2 or N_2. In the EXAFS measurements in H_2 or N_2, a drastic change of $k^3\chi$ was observed for $[Ru_6N]$−Cs^+/MgO in H_2 (Figure 6 and Table 3) compared to no change in vacuum at 30−293 K (Tables 1 and 3). Smaller changes of $k^3\chi$ (and the fitted values) were observed for $[Ru_6N]$/MgO by the introduction of H_2 (Table 3). It should be noted that initial EXAFS spectra in vacuum were reproduced by the evacuation for these two cases in H_2, indicating these EXAFS changes by the adsorption/desorption of H_2 were reversible.

The causes of the spectral changes in H_2 or N_2 were classified as (1) simple adsorption of gas and (2) adsorption-induced structure changes of cluster framework (Δr_{Ru-Ru}) and cluster/

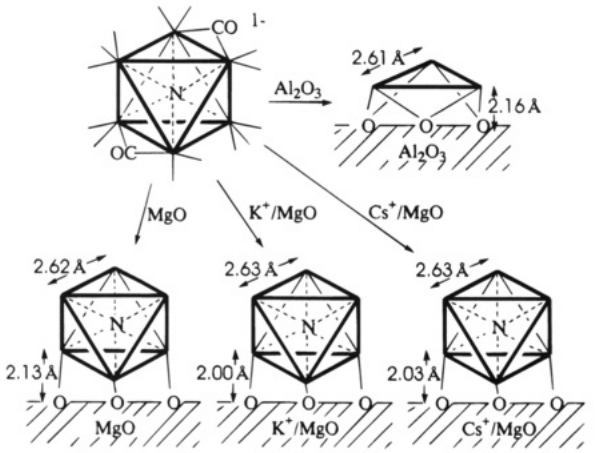

Figure 7. Structures of supported clusters on MgO, K^+/MgO, Cs^+/MgO, and Al_2O_3 prepared from $[Ru_6N(CO)_{16}]^-$. The samples were heated in vacuum (813 or 673 K) and in H_2 (588 K).

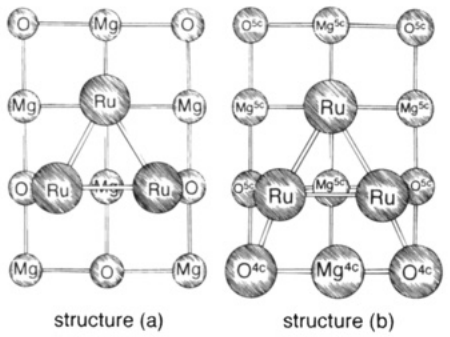

Figure 8. Structure models for $[Ru_6N]$ clusters on MgO: (a) on flat MgO face; (b) on stepped MgO face. Average $N_{Ru-O_{su}}$ are 0.5 and 0.83 in model structures (a) and (b), respectively. The $r_{Ru-O_{su}}$ are based on EXAFS data in Table 2 (2.13 for (a) and 2.09 Å for (b)). Only Ru_3 triangle faces of $[Ru_6N]$ are drawn for clarity.

support interface ($\Delta r_{Ru-O_{su}}$). The adsorption of N_2 should be simple nondissociative adsorption. Examples are reported for the distance $r_{metal-N}$ for adsorbed N_2 on metal catalysts or N_2-coordinated organometallic complexes. The r_{Ni-N} were reported to be 1.91−1.94 Å for π-coordinated N_2 in $[(PhLi)_6Ni_2N_2(Et_2O)_2]_2$.[21] The r_{V-N} were reported to be 1.832−1.833 Å for nearly straight V−N−N−V bonding in $(\mu_2\text{-}N_2)[\{(o\text{-}Me_2NCH_2)C_6H_4)\}_2V(Py)]_2(THF)_2$.[22] The r_{Ti-N} were reported to be 1.857−2.181 Å for μ_3-N_2 in $(\mu_3\text{-}N_2)[(\eta^5\text{:}\eta^5\text{-}C_{10}H_8)(\eta\text{-}C_5H_5)_2Ti_2]\cdot[(\eta^1\text{:}\eta^5\text{-}C_5H_4)(\eta\text{-}C_5H_5)_3Ti_2]\cdot[(\eta\text{-}C_5H_5)_2(C_6H_{14}O_3)Ti]\cdot C_6H_{14}O_3$.[23] The r_{Ru-N} were 1.95−2.02 Å for N_2(a) on $[Ru_6N]$/MgO and $[Ru_6N]-Cs^+$/MgO (Table 3). The adsorptions of molecular N_2 were not accompanied by the expansion/contraction of cluster framework $[Ru_6N]$, keeping the r_{Ru-Ru} (almost) unchanged for $[Ru_6N]$/MgO (2.62 Å) and for $[Ru_6N]-Cs^+$/MgO (2.64 ± 0.01 Å) (Table 3).

The adsorption of H_2 must be accompanied by adsorption-induced structure changes of cluster framework $[Ru_6N]$. The r_{Ru-Ru} changes from 2.62 to 2.65 Å for $[Ru_6N]$/MgO and from 2.63 to 2.71 Å for $[Ru_6N]-Cs^+$/MgO (Table 3) by the adsorption of hydrogen. These H-induced structure changes also induced smaller changes of cluster/support interface; the $r_{Ru-O_{su}}$ changed from 2.13 to 2.17 Å for $[Ru_6N]$/MgO and from 2.03 to 2.06 Å for $[Ru_6N]-Cs^+$/MgO (Table 3). The changes of r_{Ru-Ru} (1.1 % for $[Ru_6N]$/MgO and 3.0% for $[Ru_6N]-Cs^+$/MgO) are smaller than the $[Ru_6C]$ framework expansion/contraction induced by CO (9.1%) for $[Ru_6C]$/MgO and $[Ru_6C]/La_2O_3$ (5.7%) and comparable to that induced by CO for $[Ru_6C]/Al_2O_3$ (1.5%).[1,2]

The H-induced structure change of the Ru(0001) surface was monitored by VLEED (very low-energy LEED (low-energy electron diffraction)).[24] It was found that the first layer Ru array expanded by 1.7% in the $[1\bar{1}00]$ direction and by 0.9% in the [0001] direction by H adsorption (T_{ad} < 72 K). The other examples of H-induced structure change were reported for Co, Ni, Pd, Mo, and W single-crystal surfaces.[25] The expansions of r_{Pd-Pd} on conventional Pd/C and Pd/Al_2O_3 by hydride or carbide formation were reported by means of EXAFS.[7] The r_{Pd-Pd} increased by 2.0 and 2.4% with hydride formation and by 1.2 and 0.3% with carbide formation for Pd/C and Pd/Al_2O_3, respectively. The expansion of r_{Pd-Pd} of Pd/ZrO_2 by carbide formation was mesured during the CO disproportionation by XRD (X-ray diffraction).[26] The carbon was incorporated up to 15 atom % in Pd, and the r_{Pd-Pd} was linearly increased by up to 2.6%. The change of r_{Ru-Ru} (Δ = 0.08 Å, 3.0%) for our $[Ru_6N]-Cs^+$/MgO (Table 3) was larger than the above H-induced reconstruction of Ru(0001) surface (0.9−1.7%) or "hydrogen-absorptive" or "carbon-absorptive" supported Pd catalysts (0.3−2.6%). This large expansion of the $[Ru_6N]$ framework may be due to the fact that all the Ru atoms of $[Ru_6N(\mu\text{-}O_{su})_3]$ were exposed and able to interact with H(a). The adsorbed amount of hydrogen atoms were three to four on $[Ru_6N]$/MgO at 185 K and five to six on $[Ru_6N]-Cs^+$/MgO at 77 K.[11]

The catalytic effect of $[Ru_6C]$ expansions of $[Ru_6C]/Al_2O_3$, $/La_2O_3$, or /MgO induced by CO was discussed and summarized to afford enough space on $[Ru_6C]$ framework to dissociate H_2 molecules, and CO-associative oxygenate compounds were selectively produced on the expanded $[Ru_6C]$.[1,2] The catalytic effects of $[Ru_6N]$ expansion/contraction of $[Ru_6N]$/MgO and $[Ru_6N]^-Cs^+$/MgO induced by hydrogen adsorption/desorption are described in the accomanying paper.

Conclusions

1. Supported $[Ru_6N(\mu\text{-}O_{su})_3]$ clusters were prepared on MgO, K^+/MgO, or Cs^+/MgO from $[Ru_6N(CO)_{16}]^-$ clusters (2.5 wt % Ru). The cluster $[Ru_6N(CO)_{16}]^-$ was cleaved to the trimer $[Ru_3(\mu_2\text{-}O_{su})_3]$ on Al_2O_3 by heating at 813 K. These clusters were stable in H_2 at 588 K.

2. The $r_{Ru-O_{su}}$ were in the range 2.09−2.17 Å for $[Ru_6N]$/MgO, and they were shorter (2.00−2.07 Å) for $[Ru_6N]-K^+$/MgO and $[Ru_6N]-Cs^+$/MgO. The $[Ru_6N]$ was implied to be reacted with three O_{su} atoms bonded to K^+ or Cs^+ ions on K^+/MgO and Cs^+/MgO.

3. The $[Ru_6N]$ was suggested to inteact with lower coordination sites of the MgO surface, such as step sites, on the basis of the increase of $N_{Ru-O_{su}}$ when the Ru loadings were changed from 2.5 to 0.5 wt %.

4. The expansion and contraction of the $[Ru_6N]$ framework were observed by the hydrogen adsorption and desorption for $[Ru_6N]$/MgO (Δr_{Ru-Ru} = 0.03 Å) and $[Ru_6N]-Cs^+$/MgO (Δr_{Ru-Ru} = 0.08 Å). This expansion/contraction of the $[Ru_6N]$ framework was found to be reversible.

5. N_2 was adsorbed on $[Ru_6N]$/MgO and $[Ru_6N]-Cs^+$/MgO at 193 K at r_{Ru-N} = 1.95−2.02 Å observed by EXAFS without structural modifications of the $[Ru_6N]$ framework.

References and Notes

(1) Izumi, Y.; Chihara, T.; Yamazaki, H.; Iwasawa, Y. *J. Phys. Chem.* **1994**, *98*, 594.

(2) Izumi, Y.; Iwasawa, Y. *Chemtech* **1994**, *July*, 20.

(3) Izumi, Y.; Chihara, T.; Yamazaki, H.; Iwaswa, Y. *J. Chem. Soc., Chem. Commun.* **1992**, 1395.

(4) Izumi, Y.; Chihara, T.; Yamazaki, H.; Iwasawa, Y. *J. Am. Chem. Soc.* **1993**, *115*, 6462.

(5) Izumi, Y.; Aika, K. *Chem. Lett.* **1995**, 137.
(6) Kamper, F. W. H.; Koningsberger, D. C. *Faraday Discuss. Chem. Soc.* **1990**, *89*, 137.
(7) McCaulley, J. A. *J. Phys. Chem.* **1993**, *97*, 10372.
(8) Izumi, Y.; Hoshikawa, M.; Aika, K. *Bull. Chem. Soc. Jpn.* **1994**, *67*, 3191.
(9) Bhatia, S.; Engelke, F.; Pruski, M.; Gerstein, B. C.; King, T. S. *J. Catal.* **1994**, *147*, 455.
(10) Izumi, Y.; Liu, T.; Asakura, K.; Chihara, T.; Yamazaki, H.; Iwasawa, *J. Chem. Soc., Dalton Trans.* **1992**, 2287.
(11) Izumi, Y.; Aika, K. *J. Phys. Chem.* **1995**, *99*.
(12) Blohm, M. L.; Gladfelter, W. L. *Organometallics* **1985**, *4*, 45.
(13) Yokoyama, T.; Hamamatsu, H.; Ohta, T. *Analysis Program EXAFSH2*; The University of Tokyo, 1994.
(14) Teo, B. K. *EXAFS: Basic Principles and Data Analysis*; Springer: Berlin, 1986.
(15) Binsted, N.; Cook, S. L.; Evans, J.; Greaves, G. N.; Price, R. *J. Am. Chem. Soc.* **1987**, *109*, 3669.
(16) *Tailored Metal Catalysts*; Iwasawa, Y., Ed.; Reidel: Dordrecht, The Netherlands, 1986; p 16.
(17) Henrich, V. C. *Rep. Prog. Phys.* **1985**, *48*, 1481.
(18) Robbins, J. L. *J. Catal.* **1989**, *115*, 120.
(19) Dalla Betta, R. A. *J. Phys. Chem.* **1975**, *79*, 2519.
(20) Brown, M. F.; Gonzalez, R. D. *J. Phys. Chem.* **1976**, *80*, 1731.
(21) Kruger, C.; Tsay, Y. *Angew. Chem., Int. Ed. Engl.* **1973**, *12*, 998.
(22) Edema, J. J. H.; Meetsma, A.; Gambarotta, S. *J. Am. Chem. Soc.* **1989**, *111*, 6878.
(23) Pez, G. P.; Apgar, P.; Crissey, R. K. *J. Am. Chem. Soc.* **1982**, *104*, 482.
(24) Held, G.; Pfnür, H.; Menzel, D. *Surf. Sci.* **1992**, *271*, 21.
(25) Christmann, K. *Surf. Sci. Rep.* **1988**, *9*, 1.
(26) Maciejewski, N.; Baiker, A. *J. Phys. Chem.* **1994**, *98*, 285.

JP9502767